J. Coat. Technol. Res.
https://doi.org/10.1007/s11998-023-00862-8

Preparation and characterization of new antifouling coating based on alkyd paint modified with hydrophobic cationic biocide

Sergiy Rogalsky, Olena Moshynets, Oleg Dzhuzha, Oksana Tarasyuk, Anastasiia Hubina, Alina Madalina Darabut, Yevheniia Lobko, Iryna Morozovska, Oleksandr Protasov, Jean-François Bardeau

Received: 13 June 2023 / Revised: 17 September 2023 / Accepted: 25 September 2023

Abstract New water-immiscible cationic biocide 1-dodecylpyridinium dodecylbenzenesulfonate ($PyrC_{12}$-DBS) has been synthesized and tested as potential antifouling agent for commercial alkyd paint PP-115 (Ukraine). The modified PP-115/$PyrC_{12}$-DBS coatings containing 8% and 16% (w/w) of $PyrC_{12}$-DBS were prepared by dissolution directly of the cationic biocide into the PP-115 paint. Once the stainless steel bars were painted, the surface wettability of the coating was found to be significantly increased when modified with cationic biocide. The results of scanning electron microscopy (SEM) and energy-dispersive X-ray spectroscopy (EDX) studies indicate high homogeneity of the modified coatings. Infrared analysis revealed hydrogen bonding between ester groups of alkyd resin and pyridinium cations of $PyrC_{12}$-DBS. The plasticizing effect of the cationic biocide on the alkyd binder has also been revealed by differential scanning calorimetry analysis. According to spectrophotometric analysis data, $PyrC_{12}$-DBS has excellent resistance to leaching from protective coatings into water. Antibiofilm efficiency of $PyrC_{12}$-DBS was evaluated by assessing the capability of two biofilm-forming model strains, namely *Staphylococcus aureus* ATCC 25923 and *Pseudomonas aeruginosa* PA01, to form attached biofilms on the surface coated with modified alkyd paint. A significant decrease in biofilm metabolic activity, as well as in cell biomass, was determined for PP-115/$PyrC_{12}$-DBS (16%) coatings. The antifouling activity was evaluated by exposure to experimental substrates in freshwater (Dnipro River) for 143 days. The surface of PP-115/$PyrC_{12}$-DBS (16%) coatings showed an almost 13-fold reduction of total biomass formed by Dreissenidae mussels compared with control substrates. Overall, the obtained data indicate that the contact-active protective coatings based on water-insoluble polymer matrix and water-insoluble cationic biocide may effectively resist biofouling at relatively high biocide content.

Keywords Antifouling coating, Alkyd paint, Cationic biocide, Contact active, Biofilm

Supplementary Information The online version contains supplementary material available at https://doi.org/10.1007/s11998-023-00862-8.

S. Rogalsky (✉), O. Dzhuzha, O. Tarasyuk
Laboratory of Modification of Polymers, V.P. Kukhar Institute of Bioorganic Chemistry and Petrochemistry of the NAS of Ukraine, 50, Kharkivske shose, Kyiv 02160, Ukraine
e-mail: sergey.rogalsky@gmail.com

O. Moshynets
Department of Cell Regulatory Mechanisms, Institute of Molecular Biology and Genetics of the NAS of Ukraine, 150 Zabolotnoho str., Kyiv 03680, Ukraine

A. Hubina
Department of Polymers, Faculty of Chemical Technology, University of Chemistry and Technology (UCT) Prague, Technická 5, Prague 166 28, Czech Republic

A. M. Darabut, Y. Lobko
Department of Surface and Plasma Science, Faculty of Mathematics and Physics, Charles University, V Holešovičkách 747/2, Praha 8, Prague 180 00, Czech Republic

I. Morozovska, O. Protasov
Department of Ecological Hydrology and Water Ecosystem Management, Institute of Hydrobiology of the NAS of Ukraine, 12, Volodymyra Ivasyuka Avenue, Kyiv 04210, Ukraine

J.-F. Bardeau
Institut des Molécules et Matériaux du Mans, UMR CNRS 6283, Le Mans Université, Le Mans, France

Published online: 03 January 2024

Introduction

Biofouling is known to take place on almost any solid substrate immersed into freshwater or seawater. This process begins with the colonization of solid substrates by microfoulers (bacteria, algae, and diatoms).[1–4] Biofilms formed on marine surfaces protect microorganisms from the action of adverse environmental conditions and allow the occurrence of macrofouling by bryozoans, mollusks, crustacean, polychaeta, fungi, etc.[3,4] The best known bioadhesive system is that produced by mussels. These shellfish attach by depositing a mixture of proteins which crosslink the macromolecules between them to harden the glue.[2] It is worth noting that the attachment of macrofoulers to biofilm-free surfaces can also occur. Biofouling creates severe economic problems all over the world, leading to considerably increased operational and maintenance costs of underwater equipment and constructions. Thus, it damages several marine facilities, including oil production platforms, powerplants, industrial water inlet systems, or seawater cooled systems.[5–7] In the shipping industry, fouling organisms attached to vessel hulls promote surface corrosion and increased frictional resistance, leading to fuel consumption and loss of speed. There are high costs incurred in ship hull cleaning and repainting, as well as loss of revenue when the frequency of dry-docking operations increased.[8,9] This fouling process also accumulates a large amount of toxic macrofouling waste in landfills. Furthermore, marine biofouling promotes bio-invasion of species into environments where they were not naturally present that has an extremely negative impact on global biodiversity.[1,2] Therefore, prevention of biofouling remains one of the most important challenges in marine industry and world ecology.

The common approach to inhibiting fouling of underwater constructions in both seawater and freshwater is to cover them with protective polymer coatings containing biocides. Various kinds of biocide-based antifouling coating systems exist, depending on how biocidal additives are released into the water.[1,10] Until recently, self-polishing coatings (SPCs) based on copolymers of tributyltin (TBT) acrylate and methyl methacrylate were the most commonly used since they provide efficient antifouling resistance for at least 5-7 years.[10] In SPCs, biocidal TBT groups are bonded onto the polymer backbone by an ester linkage. After immersion, slow hydrolysis of carboxyl-TBT linkage occurs on the surface and cleaves the TBT moiety from the hydrophobic polymer matrix. The partially hydrolyzed polymer backbone becomes hydrophilic, and a surface layer can then be easily eroded by the moving seawater, leading to renewal of a bioactive surface in contact with water.[10,11] However, the use of organotin additives in marine paints was banned recently by the International Marine Organization due to their severe negative impact on nontarget species, including commercially important organisms.[12]

During the last decade, significant investments have been made in the development of tin-free antifouling systems which may be classified into the following main groups. Tin-free SPCs are based on organo copper esters of poly(methacrylic acid) copolymers which have the same biocide-releasing mechanism with seawater as TBT-SPCs.[1] The Cu-acrylate coatings have been reported to be active for up to 3 years. Controlled depletion systems (CDPs) consist of soluble binder based on synthetic resins and rosin derivatives incorporating seawater-soluble cuprous oxide.[1] Once in contact with seawater, the biocides dissolve together with the soluble binder. This type of antifouling coating is less effective for up to 36 months.[1] It should also be noted that high cuprous oxide loading (more than 40% by volume) is required to permit adequate release of copper for prolonged periods.[13] Thus, the mechanism of action of common TBT-free antifouling coatings also involves gradual wasting of their components producing a thin, toxic layer which repels aquatic organisms and therefore prevents the onset of biofouling. However, the amounts of copper leached from antifouling paints were also found to be harmful for various aquatic micro- and macroorganisms.[14–16] Meanwhile, the use of copper alone is not enough to prevent marine organisms from attaching to surfaces and it is for this reason that coatings are filled with biocides (usually pesticides) to boost their effectiveness. The toxic impact of booster biocides such as Diuron, Sea-Nine 211, Irgarol®, and zinc pyrithione on nontarget species has also been established.[17–20]

Therefore, the problem still remains and there is a need to develop alternative antifouling coatings which combine both high efficiency and low environmental impact, as well as low cost. The simplest solution would be to use a polymer matrix that is insoluble in seawater and does not polish or erode after immersion. Such antifouling coatings require sufficiently high loading of biocide to permit continuous contact of toxic particles. However, the common insoluble matrix paints also include toxic antifouling agents that are released upon contact with water. The active species dissolved by the seawater penetrating into the polymer matrix have to diffuse to the surface through the interconnecting pores formed after dissolution of the soluble pigments.[1] The short life time of these coatings (12–18 months) has limited their practical applications. So, the use of insoluble matrix paints containing water-insoluble biocides seems to be the next step in the development of new environmentally friendly antifouling coatings. Potential advantages of such systems include the absence of release of biocides into the aquatic environment, as well as long-term antifouling activity.

Nowadays, contact-active antimicrobial polymer composites are considered very promising eco-friendly materials for various applications since they do not release biocides into contact medium.[21–23] The covalent surface grafting of cationic biocides to various synthetic and natural polymers is a common approach

for the formation of safe and effective antimicrobial materials.[24] Cationic biocides based on long-chain quaternary onium salts comprising tetraalkylammonium, 1,3-dialkylimidazolium, and 1-alkylpyridinium cations are known to possess broad-spectrum activity against both gram-positive and gram-negative bacteria, antifungal activity, as well as strong antibiofilm activity against a panel of pathogen microorganisms.[25–30] The mechanism of antimicrobial action of cationic biocides involves the electrostatic interaction with outermost surface of bacterial cells which are often negatively charged and association with the head groups of acidic phospholipids. The lipophilic hydrocarbon tails of the cationic amphiphilic compound then penetrate into the hydrophobic membrane core and form mixed-micelle aggregates with its components, resulting in a deformation of membrane permeability and lethal leakage of cytoplasmic materials.[27,31,32]

Moreover, 1-dodecyl-3-methylimidazolium iodide was found to have superior antibiofouling activity against dominant fouling barnacle *Amphibalanus reticulatus*.[33] It has also been found that polymeric alkylpyridinium salts (poly-APS) isolated from the Mediterranean marine sponge, Haliclona (Rhizoniera) sarai, effectively inhibit barnacle larva settlement and natural marine biofilm formation through a nontoxic and reversible mechanism.[34] Few synthetic analogs of poly-APS showed antifouling efficacy very similar to natural ones, as well as negligible toxicity.[34]

Numerous studies have shown that cationic biocides attached covalently to the polymer surface are able to kill microorganisms at the polymer–water interface similarly to free biocide molecules in water solution.[21,24,35] These sterile-surface materials have long-lasting antimicrobial activity and effectively prevent the formation of microbial biofilms. However, the covalent grafting of biocides to the surface of protective coatings is difficult to realize from a practical point of view. At the same time, recent studies reported preparation of contact-active antimicrobial materials based on synthetic polymers (i.e., polyamides, polycaprolactone, polylactides, silicone rubber) comprising hydrophobic cationic biocides as external additives.[36–40] Polymer films containing 5–7 wt% of low molecular or polymeric cationic biocides showed a high activity against both gram-positive and gram-negative bacteria,[37–40] as well as high antibiofilm activity.[36,40] It has also been found that hydrophobic cationic biocides have excellent leaching resistance due to their poor water solubility, as well as physicochemical interactions with polymer matrix.[36,37,40] Another successful approach to prepare contact-active antimicrobial composites involves the intercalation of the cationic polymer, partially aminated poly(vinylbenzyl chloride), into a smectic clay, montmorillonite, to produce a modified organoclay containing 33 wt% of polymeric biocide.[41] Polymerically modified organoclay was compounded with polyamide resin by melt extrusion. The obtained nanocomposites were active against both gram-negative *E. coli* and gram-positive *S. aureus* bacteria and demonstrated up to a 2-log reduction in the viable cells adhering to the material surface at an organoclay content of 5 wt%. The mode of antimicrobial action of this material was determined as contact-active due to the nonleachable form of biocide.[41]

Thus, water-immiscible cationic biocides seem promising candidates as antifouling additives for ship paints. Liquid long-chain onium salts are of particular interest as they dissolve easily in paints and therefore can be used in coatings. In this study, hydrophobic cationic biocide 1-dodecylpyridinium dodecylbenzenesulfonate ($PyrC_{12}$-DBS) has been synthesized by anion metathesis between 1-dodecylpyridinium chloride and sodium dodecylbenzenesulfonate. Water-soluble 1-dodecylpyridinium salts are known to possess excellent antimicrobial activity which is significantly higher compared to quaternary ammonium surfactants,[42] as well as 1-alkyl-3-dodecylimidazolium salts[26,30,43] The combination of 1-dodecylpyridinium cation with DBS anion allowed preparing water-immiscible cationic biocide which was evaluated as potential antifouling agent for industrial ship paint. The modified protective coatings containing $PyrC_{12}$-DBS were prepared and characterized in terms of morphological, surface, and thermophysical properties, antibiofilm activity, as well as antifouling activity in freshwater environment.

Materials and methods

Materials

Pyridine (99%), 1-chlorododecane (97%), sodium dodecylbenzenesulfonate (technical grade), methylene chloride, hexane, and ethyl acetate (98%) (Sigma-Aldrich) were purchased from ALSI (Ukraine) and used without further purification.

Commercial paint PP-115 (Sorbi, Ukraine) was used for the preparation of protective coatings. The paint contains a mixture of pigments and fillers (calcium carbonate, titanium dioxide, iron oxide) in an alkyd (pentaphthalic) varnish. Mass fraction of nonvolatile substances is about 60 ± 10%.

Synthesis of cationic biocide 1-dodecylpyridinium dodecylbenzenesulfonate ($PyrC_{12}$-DBS)

1-Dodecylpyridinium chloride ($PyrC_{12}$-Cl) was synthesized according to Scheme 1. The mixture of pyridine (20 g, 0.24 mol) and 1-chlorododecane (59 g, 0.29 mol) was stirred at 140°C for 24 h. The obtained solid product was purified by recrystallization from ethyl acetate–hexane mixture (1:2 v/v). Yield: 72% (48 g), white solid, mp 92–94°C.

^{1}H NMR (400 MHz, $CDCl_3$): δ = 0.75 (t, J = 6.8 Hz, 3H, CH_3), 1.14-1.41 (m, 18H, $CH_3(CH_2)_9$), 1.91 (p, J = 7.4 Hz, 2H, NCH_2CH_2), 4.87 (t, J = 7.4 Hz, 2H, NCH_2), 8.06 (t, J = 6.9 Hz, 2H, C_3–H, C_5–H), 8.39 (t,

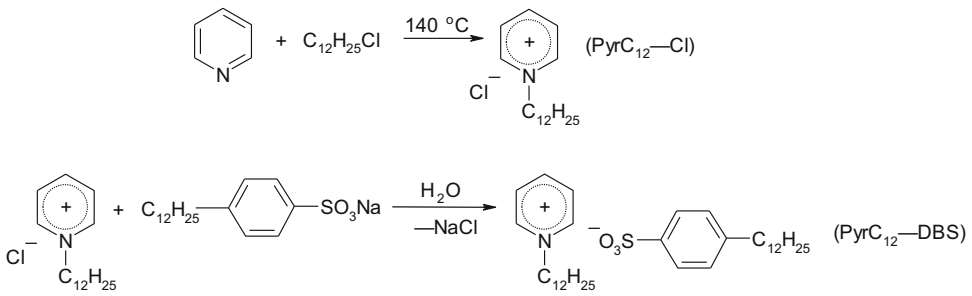

Scheme 1: Synthesis of cationic biocide $PyrC_{12}$-DBS

J = 7.8 Hz, 1H, C_4–H), 9.56 (d, J = 5.9 Hz, 2H, C_2–H, C_6–H).

To the stirred solution of $PyrC_{12}$-Cl (20 g, 0.07 mol) in 200 mL of water was added aqueous solution of sodium dodecylbenzenesulfonate (24 g/300 mL). The mixture was stirred for 1 h, and then, the product was extracted with methylene chloride (2 × 250 mL). The combined solution was dried over sodium sulfate. Methylene chloride was then distilled, and the residual solvent was removed under vacuum (10 mbar) at 50°C for 12 h. Cationic biocide $PyrC_{12}$-DBS was prepared as a light brown semi-solid product.

^{1}H NMR (400 MHz, $CDCl_3$): δ = 0.68-0.91 (m, 9H, CH_3); 0.96-1.34 (m, 32H, CH_2); 1.39-1.69 (m, 4H, CH_2); 1.89 (p, J = 7.2 Hz, 2H, NCH_2CH_2); 4.76 (t, J = 7.4 Hz, 2H, NCH_2); 7.08-7.17 (m, 2H, C_3-Ar-H, C_5–Ar–H); 7.77 (dd, J = 8.3, 1.9 Hz, 2H, C_2–Ar–H, C_6–Ar–H,); 8.0 (dd, J = 7.8, 6.4 Hz, 2H, C_3–H, C_5–H); 8.36 (t, J = 7.8 Hz, 1H, C_4–H); 9.08-9.16 (m, 2H, C_2–H, C_6-H).

Preparation of antifouling coating

Stainless steel bars (8 × 2.5 × 0.05 cm) were used as model substrates for testing the antifouling coating. Cationic biocide $PyrC_{12}$-DBS was added to the commercial ship paint PP-115 (5% and 10% (w/w) to wet paint or 8% and 16% (w/w) to dry coating), and the mixture was ground using zirconia grinding media for 30 min. The modified paint was then filtered and used to paint the steel bars using a paint roller. After drying for 48 h in air, the samples were coated with a second layer. The total coating thickness was about 300 ± 10 μm. The total weight of coating was determined by weight difference between painted and neat steel bars. The control samples were coated with two layers of paint PP-115.

Characterization of prepared coatings

The vibrational properties of protective coatings were studied using a Vertex-70 Bruker (Germany) Fourier transform infrared (FT-IR) spectrometer equipped with a DTGS detector. Coating samples were placed into contact with the single reflection diamond ATR (attenuated total reflection) crystal, and the spectra were collected over the range of 400–4000 cm^{-1} at a resolution of 1 cm^{-1}.

In order to study the surface chemical modifications of coatings with higher spatial resolution, Raman measurements were taken at room temperature using a WITec Alpha 300R confocal Raman spectrometer (WITec GmbH, Ulm Germany). Raman spectra were acquired in backscattering under a microscope with a Zeiss EC Epiplan-Neofluar® 100X objective (numerical aperture of 0.9) focusing the 532-nm line of a solid-state sapphire laser (Coherent Inc., Santa Clara, USA) with a laser power at the sample of 8 mW and an integration time set at 1 s. The spectrometer being equipped with a motorized scanning stage, 1600 spectra were recorded from a mapping area of 40 × 40 μm^2 (2D map step size of 1 μm). The spectral analysis was performed using the WITec Project plus software (version 5.248, WITec GmbH, Germany).

The adhesion of the coating onto the substrates was determined in accordance with ASTM D 3359, method B. Latticed notches were applied to the finished coatings followed by visual assessment of its condition. The adhesion for all coatings was 1 point (5 B). The edges of cuts were completely smooth, and there were no signs of delamination on all edges of the lattice.

Static contact angle measurements were taken using a Drop Shape Analyzer DSA25E (Krüss, Germany) by the sessile drop method. The contact angle values were estimated, using CAM software, as the tangent normal to the water drop (3 mL) at the intersection between the sessile drop and the polymer coating surface. All reported contact angles are the average of at least five measurements taken at different locations on the polymer surface.

The 3D surface topography of the coatings was studied using the confocal white-light optical imaging S-NEOX profiler (Sensofar-Tech S. L., Barcelona, Spain). The 340 × 284 μm^2 area was collected using a 50 X DI Nikon objective (0.8 numerical aperture). The data were analyzed by the open-source Gwyddion software (version 2.60).

Scanning electron microscopy (SEM) images were taken using a MIRA 3 (Tescan GmbH, Czech Republic) microscope operating at 10 kV electron beam energy. Chemical composition mapping analysis was carried out using energy-dispersive X-ray spectroscopy

(EDX) with a Bruker XFlash detector mounted directly into the SEM.

Differential scanning calorimetry (DSC) analyses were performed from − 90 to 100°C on a Discovery DSC250 Auto (TA Instruments, USA) with a heating rate of 10°C/min under N_2 atmosphere. The data for analysis were acquired from the second heating run.

The release of $PyrC_{12}$-DBS from the coatings was studied by UV–visible spectrophotometric analysis using a Jenway 6850 spectrometer (Great Britain). The calibrating graph was obtained by measuring the absorbance at 259 nm (characteristic peak of pyridinium cation[44]) of $PyrC_{12}$-Cl aqueous solutions in a concentration range of 1.5×10^{-5}–1.5×10^{-4} mol/L. For the evaluation of the leaching rate of cationic biocide, each painted steel bar (three samples) was placed into a closed conical flask containing 1 L of deionized water. The samples were kept at 25°C. Three milliliters of each solution was taken periodically and analyzed by measuring the absorbance at mentioned wavelength to determine the concentration of the released biocide. Each measurement was repeated three times.

Antibiofilm efficiency of $PyrC_{12}$-DBS was evaluated by assessing the capability of two biofilm-forming model strains, *Staphylococcus aureus* ATCC 25923 and *Pseudomonas aeruginosa* PA01, to form attached biofilms on the surface coated with PP-115 and PP-115/$PyrC_{12}$-DBS following two days of stationary incubation. For this, 1 cm^2 metal plates covered with either PP-115 or PP-115/$PyrC_{12}$-DBS were sterilized by autoclaving at 105°C for 30 min. Each substrate was then placed in a well of a sterile polystyrene 24-well plate in which 2 mL of Luria broth (LB) medium was added and inoculated with 10 µL of an overnight inoculum culture containing 10^9 CFU/ml; there were six replicas per variant. The plate was incubated at 37°C for 48 h. The control for incubation was performed by incubating the substrates in sterile LB with four replicas. After incubation, each sample was removed and washed three times to remove planktonic and poorly attached biofilm mass. To measure the level of total biofilm metabolic activity, MTT assay was performed. To this end, six substrates with attached biofilms for each strain were placed in a new sterile polystyrene 24-well plate, and 200 µL 0.05% MTT (3-(4,5-dimethylthiazol-2-yl)− 2,5-diphenyltetrazolium bromide; Sigma-Aldrich, UK) in LB was added to each sample and incubated at 37°C for 2 h, LB-MTT medium was sedimented at 10,000 g for 10 min, the sediment was resuspended in 200 µl DMSO, and also, 200 µL DMSO was added to each sample. Out of the final 400 µL of DMSO-dissolved formazan solution per sample, 100 µL was transferred to a polystyrene 96-well plate, and metabolic activity (A 570) was measured using a Multiskan FC Microplate Photometer (ThermoFisher Scientific, Waltham, MA, USA).

Biofilms formed onto PP-115- and PP-115/$PyrC_{12}$-DBS-coated substrates were also investigated by confocal laser scanning microscopy as it was done before.[45] The biofilms were stained with 1 mM ethidium bromide (Sigma-Aldrich) and 5 µg/mL calcofluor white solution (Sigma-Aldrich). No additional washing was used in order to limit the physical disruption of biofilm structures through liquid movement. The samples were not fixed, and a cover slip was placed over the stained samples before imaging. CLSM analysis was undertaken using a Leica TCS SPE confocal system with coded DMi8 inverted microscope (Leica, Germany) and Leica Application Suite X (LAS X) version 3.4.1. Images were acquired using excitation at 405 nm and emission collected at 450–500 nm for calcofluor white, and excitation at 532 nm and emission collected at 537–670 for ethidium bromide. The total pixels were calculated by the above-mentioned software.

Replicate data were processed using the statistical software package OriginPro 7.0 and MS Excel for Windows. All results are presented as the mean ± standard deviation. A value of $p < 0.05$ was considered statistically significant.

For biofouling testing, the painted stainless steel bars were fixed on experimental stand with the help of corrosion-resistant wire. Each series contained 12 samples. The stand with experimental substrates was dipped into water of Kaniv reservoir of the Dnipro River to a depth from 1 to 1.5 m. During the experiment sample, selections were carried out for 35 and 143 days. Removed substrates were fixed by 4% (w/w) formaldehyde solution for the following laboratory studies. The number (exemplars (ex)/m^2) and biomass (g/m^2) of hydrobionts was determined using the standard method.[46]

Results and discussion

IR analysis

Infrared spectroscopy was used both to confirm the presence of cationic biocide $PyrC_{12}$-DBS inside the coating and to reveal and identify specific interactions between PP-115 based on alkyd resin and the biocide.

In the IR spectrum of $PyrC_{12}$-DBS (Fig. 1), the strong bands in the 2800–3000 cm^{-1} region are associated with the alkyl chain of the compound. In particular, the band at 2923 cm^{-1} is attributed to the CH_2 asymmetric stretching mode and the band at 2853 cm^{-1} to CH_2 symmetric stretching mode. The two smaller intensity bands, observed at 2955 cm^{-1} and 2872 cm^{-1}, are assigned to the asymmetric and symmetric stretching vibrations of the methyl group.[47–49] The weak bands at 1635 and 1600 cm^{-1} are assigned to aromatic C=C stretching vibrations, the sharp peaks at 1489 and 1467 cm^{-1} to CH_2 bending vibrations,[47,50] and the bands at 1460 and 1377 cm^{-1} to asymmetric and symmetric bending vibrations of CH_3 groups.[48] In the region 1150–1260 cm^{-1}, the intense asymmetric broad band can reasonably be refined using five different vibrational modes assigned to aromatic C–H

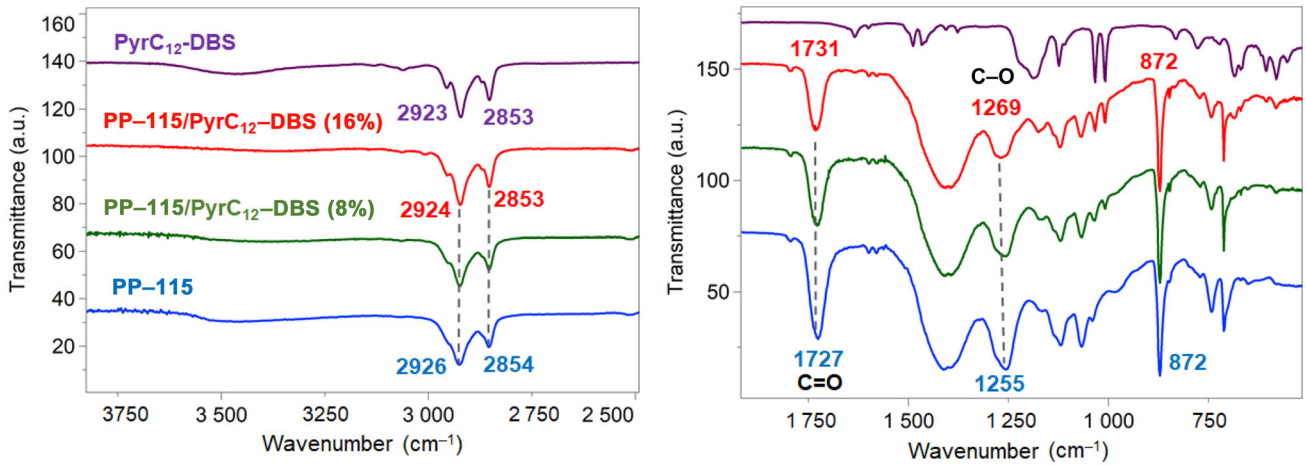

Fig. 1: IR spectra of cationic biocide and coatings based on alkyd resin

wagging (at 1227 cm^{-1}), C–N–C symmetric stretching vibrations (at 1192 cm^{-1}), asymmetric stretching vibrations of S=O group (at 1212 and 1177 cm^{-1}), and a combination of C–S stretching and alkyl C–C symmetric stretching vibrations (at 1160 cm^{-1}).[51,52] The asymmetric band at 1124 cm^{-1} is attributed to a combination of the benzene ring breathing vibration and SO_3 stretching mode.[51,52]

IR spectrum of control coating PP-115 based on alkyd resin (Fig. 1) contains a broad band with low absorption in the region 3600-3400 cm^{-1}, assigned to stretching vibrations of hydrogen-bonded hydroxyl groups.[53] This indicates the presence of a small number of unreacted OH groups of the free pentaerythritol in the polymer binder. In the high wavenumber region, the bands at 2926 and 2854 cm^{-1} are assigned to CH_2 asymmetric and symmetric stretching vibrations, respectively. The strong band at 1727 cm^{-1} is assigned to the stretching vibrations of C=O groups and the observation of an asymmetric broad bands between 1370 and 1500, and two well-defined bands at 872 cm^{-1} and 711 cm^{-1} confirm the presence of $CaCO_3$ polymorph.[54,55] These bands are commonly attributed to the asymmetric stretching modes and the asymmetric and symmetric deformations of the calcite, respectively.[56] However, the band at 711 cm^{-1} being asymmetrical with a shoulder around 700 cm^{-1}, the presence of an aragonite phase in the paint cannot be excluded. Finally, the absorption band at 1255 cm^{-1} indicates the presence of C–O stretching vibrations of ester groups, while the bands at 1120 and 1067 cm^{-1} are assigned to the stretching vibrations of C–O bonds from free OH groups.[53]

A comparison of the IR spectra of pure PP-115 paint and PP-115/$PyrC_{12}$-DBS (16%) reveals that the characteristic peak of the carbonyl band shifts by 4 cm^{-1} to higher frequencies concomitantly with a significant shift from 1255 to 1269 cm^{-1} of the C–O stretching mode of the ester groups. The peak position associated with the deformation of $CaCO_3$ not being impacted by the introduction of the cationic biocide, we compared

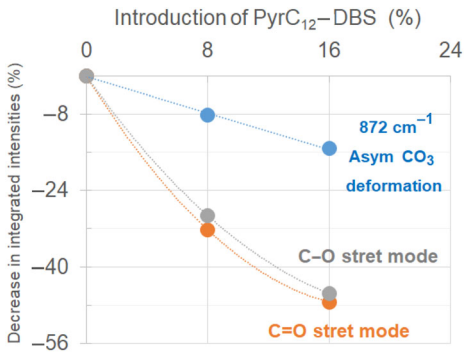

Fig. 2: Evolution of integrated intensities of asymmetric CO_3 deformation, C=O and C–O stretching modes with the introduction of $PyrC_{12}$-DBS content

the loss of integrated intensity of this mode, with those associated with the C = O and C–O stretching modes (Fig. 2). While the intensity loss follows a linear law for the $CaCO_3$ deformation mode, in accordance with the introduction of 8 and 16% of biocide, the intensity loss for the other two modes is similar and much faster, confirming strong physicochemical interactions with these functional groups. C–H bonds in ortho-position of pyridinium cation being slightly acidic due to the lowest electron density on carbon atoms,[57] hydrogen bonding may thus occur between C–H groups of $PyrC_{12}$-DBS and carbonyl oxygen of ester groups carrying partial negative charge (Scheme 2).

Morphological and surface properties

Surface roughness is known to promote water organism settlement since it creates appropriate attachment points for bioadhesion.[9] Thus, smooth surfaces are considered much more resistant to biofouling.[3,9] The 3D surface topography of the PP-115-based coatings was studied using a confocal white-light optical imag-

ing profiler (Fig. 3). The root mean square roughness Sq describes the root mean square average of height deviations taken from the mean data plane and the average roughness Sa describes the difference in height of each point compared to the arithmetical mean of the surface. These values determined on the same surface dimension (340 × 284 μm^2) are similar, which shows that the introduction of the biocide does not modify the surface roughness. Overall, the prepared PP-115/PyrC$_{12}$-DBS coatings can be considered smooth since their surface roughness is only twice that of commercial silicone-based marine coating.[3]

To quantitatively assess the variation in wettability of the surface of the films induced by the introduction of biocide, static water contact angle measurements were taken. The results are illustrated in Fig. 4. The surface of neat PP-115 coating has water contact angle (θ_ω) of 100°, which indicates high hydrophobicity.[58] Modified PP-115/PyrC$_{12}$-DBS coatings showed significantly higher wettability which is manifested by a strong decrease of θ_ω values (Fig. 4). This effect is probably due to the predominant orientation of the polar groups of the cationic biocide on the surface of the polymer matrix, thus allowing the formation of a hydration layer by means of hydrogen bonding between the water molecules and 1-dodecylpyridinium salt. This wettability is significant enough to reduce the adhesion of proteins to the surface and then the initial attachment and subsequent accumulation of fouling organisms.[59–61]

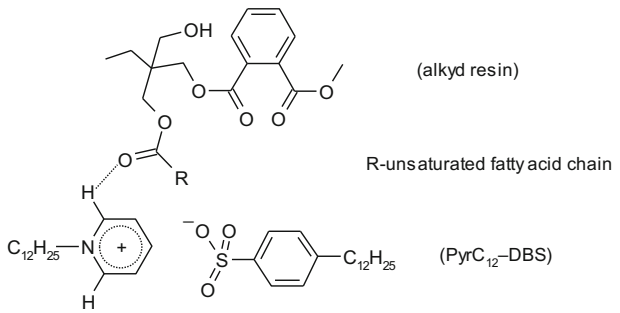

Scheme 2: Hydrogen bonding between alkyd resin and cationic biocide

Raman imaging

In order to localize the chemical modifications of the coating surfaces after introduction of the biocide, Raman spectra were recorded for each sample over an area of 40 × 40 μm^2 (2D map step of 1 μm) and a true component analysis (TCA) was performed. This dedicated tool of the WITec Project FIVE plus software helps to identify pixels in a map with similar spectral features and provide these spectral characteristics (i.e., similar chemical response) in an image of

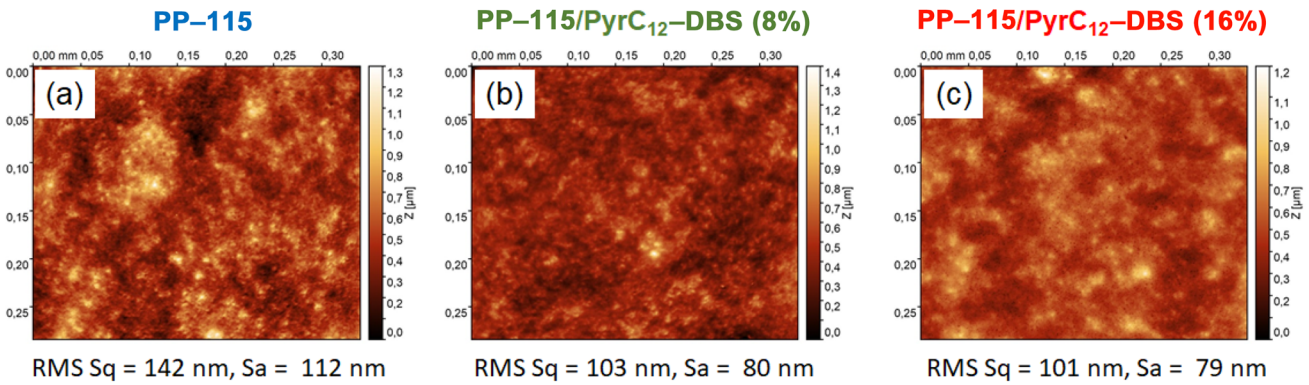

Fig. 3: 2D topographical images obtained with an optical confocal profiler: (a) control PP-115 coating, (b) modified PP-115/PyrC$_{12}$-DBS (8%) coating, and (c) modified PP-115/PyrC$_{12}$-DBS (16%) coating. The root mean square roughness (RMS) Sq and the arithmetic mean roughness Sa are given below each image

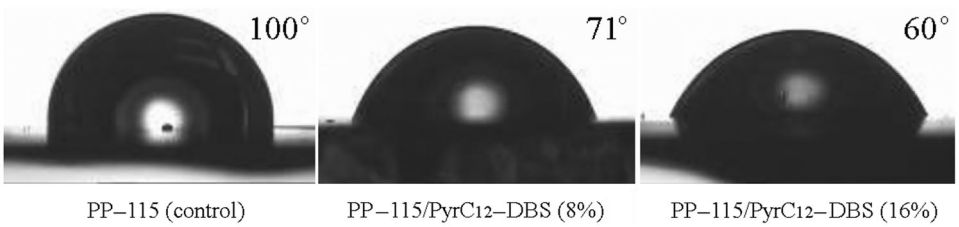

Fig. 4: Photographs of water droplets on the surface of coatings

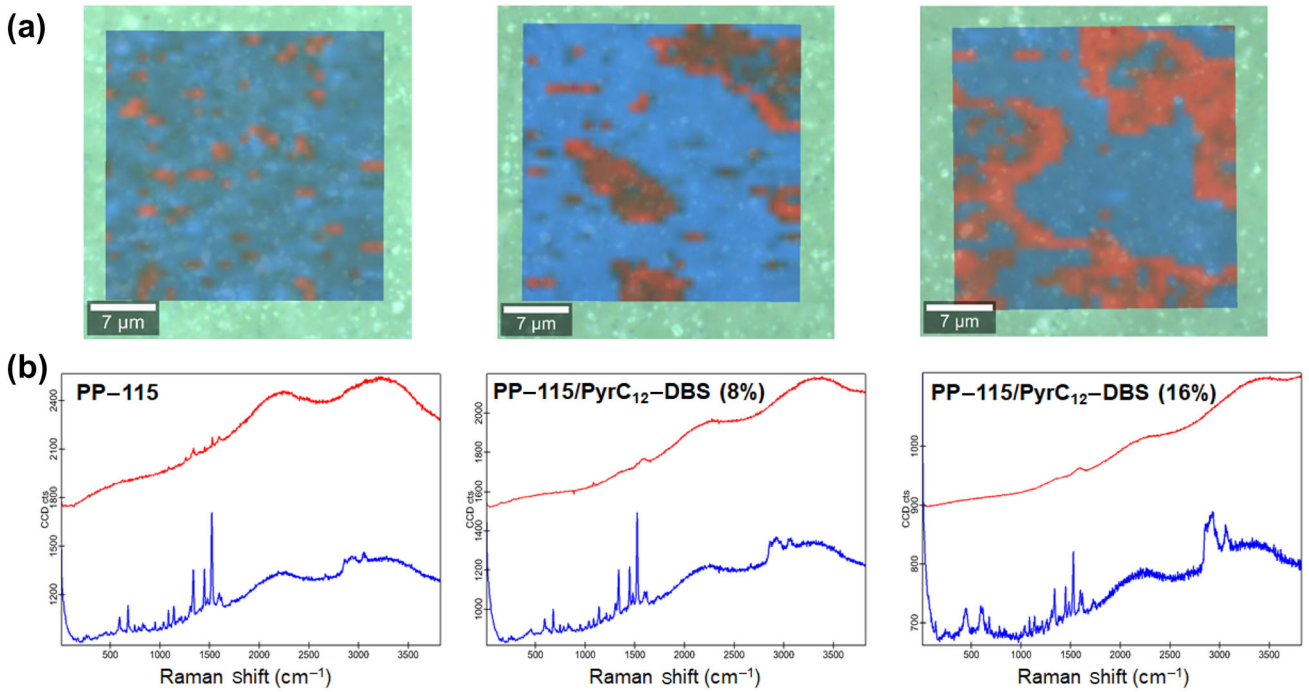

Fig. 5: Raman mapping based on 1600 spectra recoded in 40 × 40 µm^2 area. (a) True component analysis identified two major spectral components for both samples. The identified components are shown in (b). For clarity, all Raman spectra were shifted in intensity

intensity distribution (Fig. 5). The spectral signatures coded in blue (component 1) can be attributed to the average spectrum of the alkyd (pentaphthalic) varnish. The second component (coded in red) is characterized by a strong luminescence whose surface proportion increases with the introduction of the biocide. This 2D representation reveals the chemical inhomogeneity of the surface. In the case of the PP-115 paint, the red areas represent 8% of the total surface likely due to the presence of pigments and/or fillers. This proportion increases to about 20% and 40% with the introduction of 8 wt% and 16 wt% of biocide, respectively, thus suggesting that the composition of the film is not homogeneous in the thickness and that an increasing part of biocide is found on the surface during drying. This result could then explain the strong decrease in the contact angle with water when the content of biocide is increased and thus the modification of the surface properties.

EDX imaging

The distribution of the biocide in the coating was evaluated by means of energy-dispersive X-ray spectroscopy (EDX). As a reference element to evaluate the homogeneity of biocide distribution, sulfur was selected as it is present in biocide counterion and is absent in the content of neat PP-115 paint, which is confirmed by the results presented in Fig. S1 and Table S1.

Figure 6 shows the distribution of sulfur (S) in all samples. Images, as well as element analysis, show the absence of sulfur in the neat paint, while both samples with biocide demonstrate noticeable sulfur content. Overall, the results of SEM and EDX analysis indicate high homogeneity of modified coatings, as well as homogeneous distribution of the elements in the bulk of samples (Fig. S2).

DSC analysis

Influence of the $PyrC_{12}$-DBS content on the T_g value of PP-115 was investigated via DSC method. On the thermogram of the cationic biocide $PyrC_{12}$-DBS (Fig. 7a), T_g is observed at − 68°C, crystallization occurs at − 13°C, and then, melting point occurs at 5°C. PP-115 demonstrates T_g around 3°C, and also, each of the composites, PP-115/$PyrC_{12}$-DBS (8%) and PP-115/$PyrC_{12}$-DBS (16%) exhibits only one T_g, at − 10°C and − 17°C, respectively (Fig. 7b). No other phase transitions can be observed on the thermograms of the composites, which indicates that no phase separation occurred, and the paint formed with the additive a homogeneous mixture. Moreover, T_g value decreases with the growth of $PyrC_{12}$-DBS content, which shows that the additive, presumably, serves as a plasticizer.

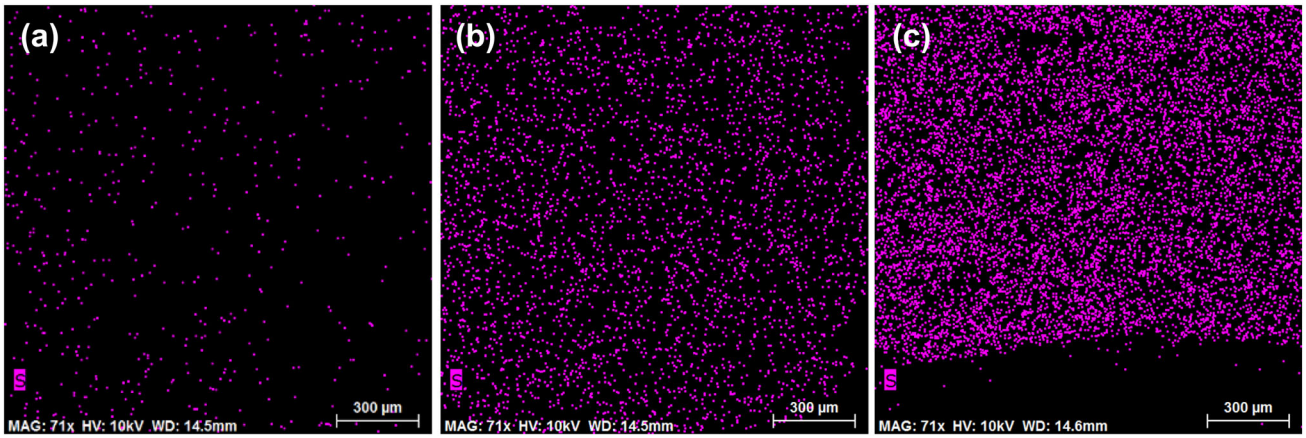

Fig. 6: Energy-dispersive X-ray spectroscopy elemental maps (S) in PP-115 (a), PP-115/PyrC$_{12}$-DBS (8%) (b), and PP-115/PyrC$_{12}$-DBS (16%) (c) coatings

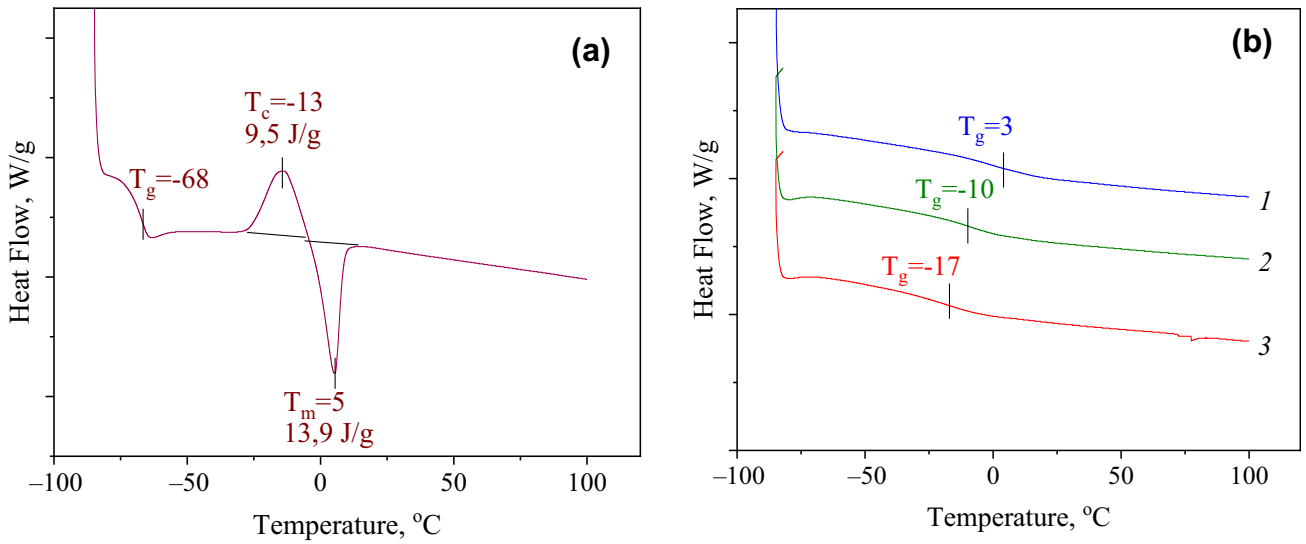

Fig. 7: DSC curves: (a) PyrC$_{12}$-DBS, (b) 1—PP-115 (control), 2—PP-115/PyrC$_{12}$-DBS (8%), 3—PP-115/PyrC$_{12}$-DBS (16%)

Leaching resistance of PyrC$_{12}$-DBS

UV–visible absorption spectroscopy is a convenient method to determine the concentrations of onium salts in water. Specifically, pyridinium salts with conjugated cation are easily detectable.[44] The results of spectrophotometric study of biocide release from PP-115 coating are illustrated in Fig. 9. UV spectrum of PyrC$_{12}$-Cl, which is water-soluble precursor for the synthesis of PyrC$_{12}$-DBS, contains two intensive peaks at 214 and 259 nm (Fig. 8, curve 1). These peaks are assigned to n–π * and π–π* electronic transitions of pyridine ring. The calibrating graph was found to be linear in the concentration range of 1.5×10^{-5}–1.5×10^{-4} mol/L at λ_{max} 259 nm. However, no signal of pyridinium cation was detected in water solution after its 60-day contact with PP-115/PyrC$_{12}$-DBS-coated steel panel (Fig. 8, curve 2). The obtained results indicate a high resistance of the cationic biocide to leaching from the protective coating which in turn is important for the potential durability of the antifouling activity of the coating, as well as for its minimal environmental impact.

Antibiofilm activity of PP-115/PyrC$_{12}$-DBS coatings

Biofilms are microbial-derived sessile communities, characterized by cells that are irreversibly attached to a surface, an interface, or to each other.[62] The microbial cells are embedded in a matrix of self-produced extracellular polymeric substances (EPS) and exhibit far more resistance to adverse environmental conditions, as well as antimicrobial agents. Therefore, understanding the mechanisms of biofilm formation is of fundamental importance to develop innovative methods to prevent biofilm growth and/or to remove

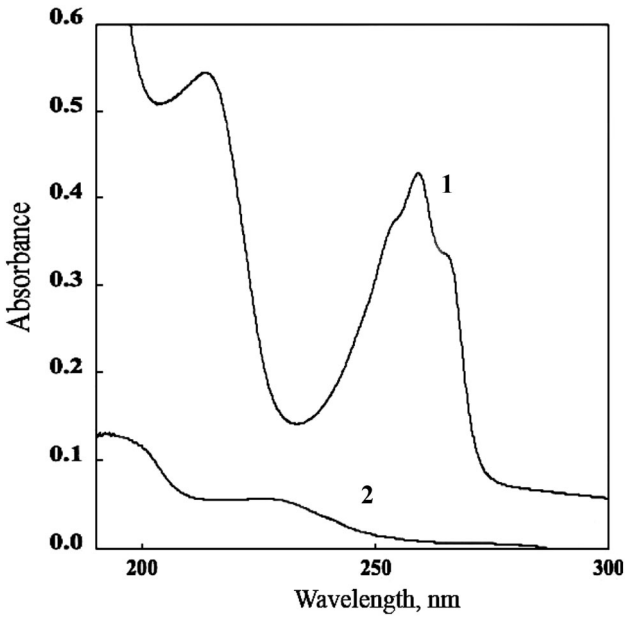

Fig. 8: UV spectra of $PyrC_{12}$-Cl (1) (C = 1 × 10^{-4} mol/L) and water solution after 60-day contact with PP-115/$PyrC_{12}$-DBS (16%)-coated substrate (2)

established biofilms. Most of the antibiofilm strategies that are currently used involve inhibition of bacterial adhesion to the surface and bacterial colonization,[3,63,64] interference with the signal molecules that modulates biofilm development,[65] and disaggregation of the biofilm matrix.[61,65] Although several strategies have been realized to deter bioadhesion, biocides, by far, still provide the most effective prevention of biofouling.[1–3]

The capability of both PP-115 and PP-115/$PyrC_{12}$-DBS to be biofouled was investigated using two standard bacterial strains *S. aureus* ATCC 25923 and *P. aeruginosa* PA 01. For this, the total metabolic activity of the 48-hour biofilms developed onto tested surfaces was measured (Fig. 9). For both gram-positive and gram-negative tested cultures, a significant drop in the metabolic activity was observed.

The decrease in biofilm metabolic activity correlated with the decrease in cell biomass observed microscopically (Figs. 10, 11). Interestingly, the $PyrC_{12}$-DBS (16%) influenced the biofilm matrix structure reducing polysaccharide content in both biofilms.

It should be noted that PP-115/$PyrC_{12}$-DBS (8%) coatings did not demonstrate noticeable antibiofilm activity (not shown in figures). Thus, the obtained results confirm the fact that the high loading of nonleaching biocide is required to prepare contact-active antibacterial surfaces.[21,35,40,41] Probably, good compatibility of $PyrC_{12}$-DBS with alkyd matrix leads to immobilization of essential part of biocide in the bulk of the resin, thus decreasing its efficient concentration at the surface.

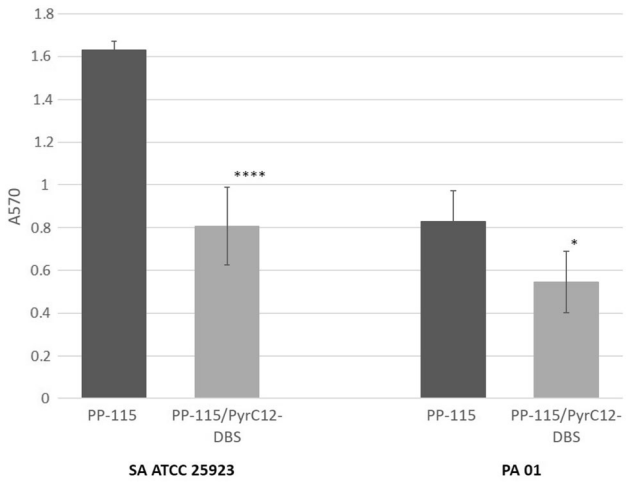

Fig. 9: The level of metabolic activity of *S. aureus* ATCC 25923 (left) and *P. aeruginosa* PA 01 (right) biofilms formed onto PP-115 (control) and PP-115/$PyrC_{12}$-DBS (16%)-coated substrate following 48 h of incubation determined by MTT staining and measured as the optical density at 570 nm (OD570). Statistical significance compared to control (no XXX added), * $p < 0.05$, **** $p < 0.001$

Antifouling activity of PP-115/$PyrC_{12}$-DBS coating

Figure 12 shows a photograph of experimental substrates after their exposure in the Dnipro River for 143 days. The surface of control coating (neat PP-115) contained 11 defined lower taxons (DLT). The total number of DLT was 52667 ± 4345 ex/m^2 which formed a biomass value of 5891 g/m^2 ± 613 g/m^2. The biofouling was determined mainly by *Dreissena polymorpha* (54% by number and 93% by mass). The surface of steel bars coated with PP-115/$PyrC_{12}$-DBS (16%) was found to have much higher biofouling resistance (Fig. 12) and contained ten DLT with a total number of 2559 ± 320 ex/m^2 and a biomass value of 430 g/m^2 ± 51 g/m^2. Similar to the control samples, *Dreissena polymorpha* formed the majority of fouling biomass (59% by number and 98% by biomass).

Thus, after 4.5-month exposure in freshwater the surface of coatings containing cationic biocide $PyrC_{12}$-DBS had more than an order of magnitude less fouling biomass compared to the control substrates. It should be noted that no difference was observed for antifouling activity of control PP-115 coatings and PP-115/$PyrC_{12}$-DBS coatings with 8% biocide content (not shown). These data agree with previously reported ones which indicate that relatively high content of water-immiscible biocide in the coating is required to impart its resistance to biofouling.[66,67] However, the question still remains about the durability of such coatings since they are often considered to be self-deactivating, because killed fouling organisms may adhere to the active layer and therefore deactivate it.[35]

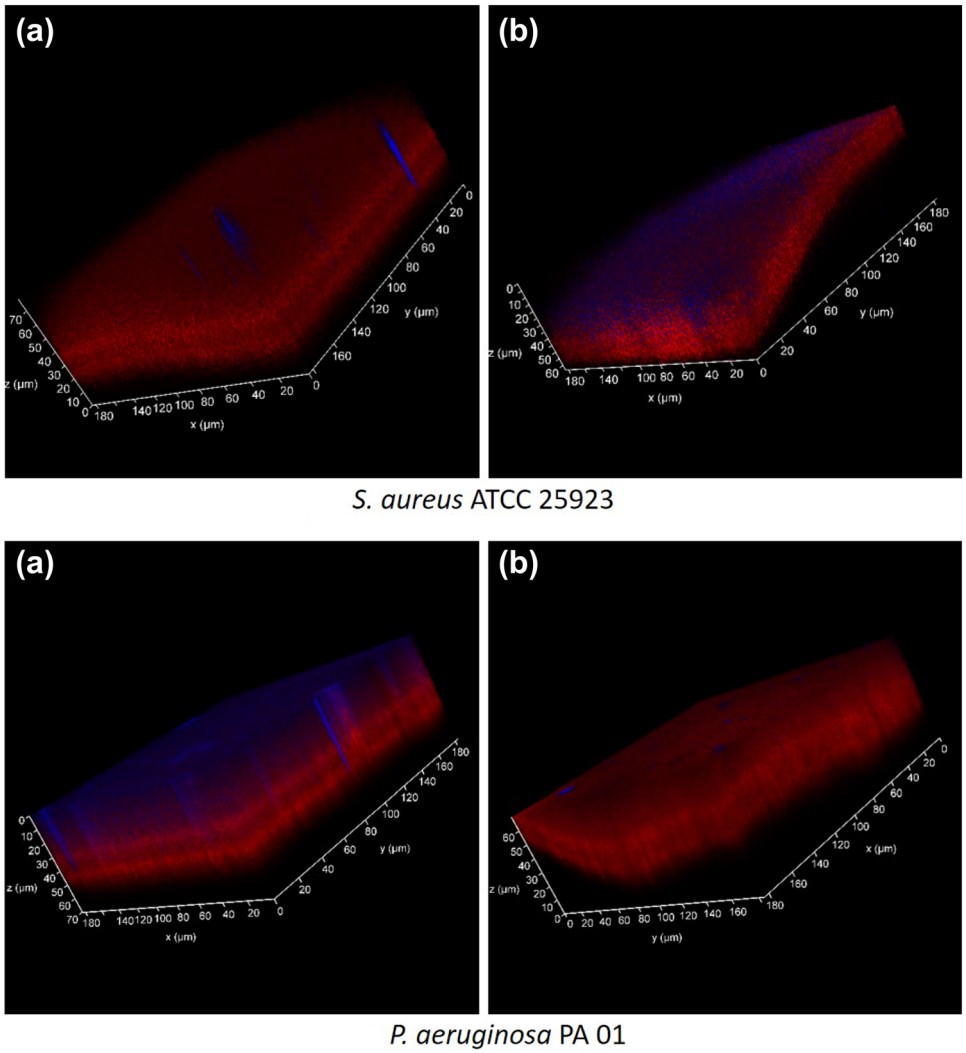

Fig. 10: CLSM imaging of *S. aureus* ATCC 25923 and *P. aeruginosa* PA 01 biofilms formed onto PP-115-coated (a) and PP-115/PyrC_{12}-DBS (16%)-coated (b) substrate following 48 h of incubation. Ethidium bromide (red signal) was used to visualize cells, and calcofluor (blue signal) was used to visualize biofilm-associated carbohydrates (Color figure online)

Conclusions

Water-immiscible cationic biocide 1-dodecylpyridinium dodecylbenzenesulfonate (PyrC_{12}-DBS) has been synthesized by anion metathesis between water-soluble precursor 1-dodecylpyridinium chloride and sodium dodecylbenzenesulfonate. PyrC_{12}-DBS has been evaluated as a potential antifouling additive for commercial alkyd paint PP-115. Thus, modified PP-115/PyrC_{12}-DBS coatings containing 8 and 16 wt% of PyrC_{12}-DBS were prepared by direct dissolution of cationic biocide in the paint followed by painting of the stainless steel bars. The results of energy-dispersive X-ray spectroscopy (EDX) study revealed homogeneous distribution of the biocide in the coatings. The analysis of 3D surface topography of the coatings by a confocal white-light optical imaging profiler has shown that the introduction of PyrC_{12}-DBS does not modify the surface roughness. The surface wettability of PP-115 coating was found to be significantly increased when modified with cationic biocide that was manifested in a sharp reduction of water contact angle. IR analysis revealed physicochemical interaction between ester groups of alkyd binder and PyrC_{12}-DBS mainly via hydrogen bonding. Moreover, the plasticizing effect of the cationic biocide on the alkyd binder has been revealed by differential scanning calorimetry. According to results of spectrophotometric analysis, no signal of 1-dodecylpyridinium cation was detected in water after 60-day contact with PP-115/PyrC_{12}-DBS coatings. This indicates excellent resistance of biocidal additive to leaching.

Antibiofilm activity of PP-115/PyrC_{12}-DBS coatings was evaluated against two biofilm-forming model strains, *Staphylococcus aureus* ATCC 25923 and *Pseudomonas aeruginosa* PA01. The decrease in biofilm metabolic activity, as well as in cell biomass attached to the surface was determined only for PP-115/PyrC_{12}-

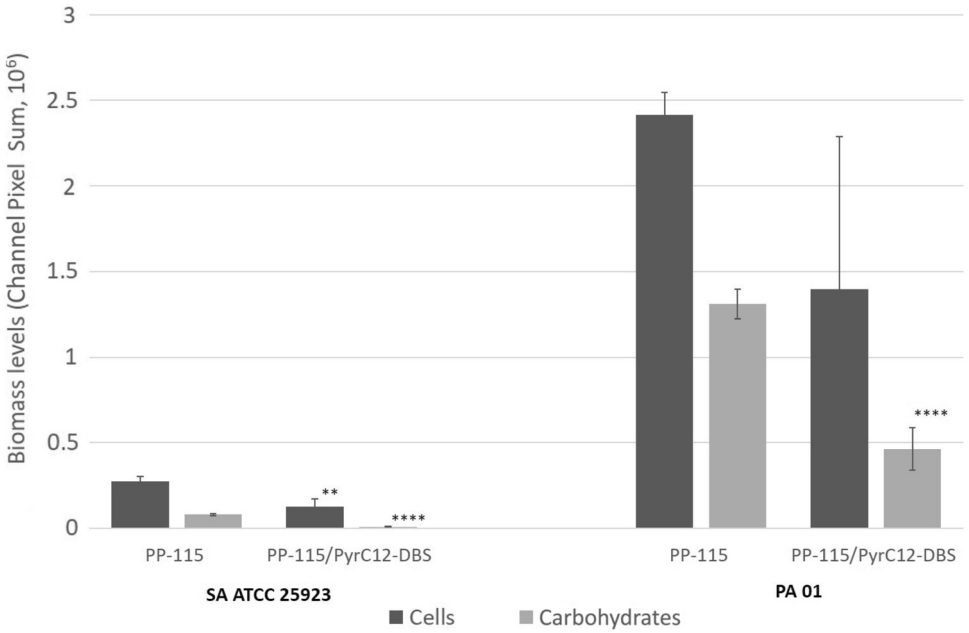

Fig. 11: The level of cell biofilm biomass (dark gray) and carbohydrate biofilm matrix (light gray) of *S. aureus* ATCC 25923 and *P. aeruginosa* PA01 biofilms formed onto PP-115-coated (control) and PP-115/PyrC$_{12}$-DBS (16%)-coated substrate following 48 h of incubation determined as the corresponding channel pixel sum calculated from the Fig. 10, where the cell biofilm biomass was tagged by ethidium bromide (red signal) and the carbohydrate biofilm matrix was tagged by calcofluor white (blue signal). Statistical significance compared to control, ** $p < 0.01$, **** $p < 0.001$

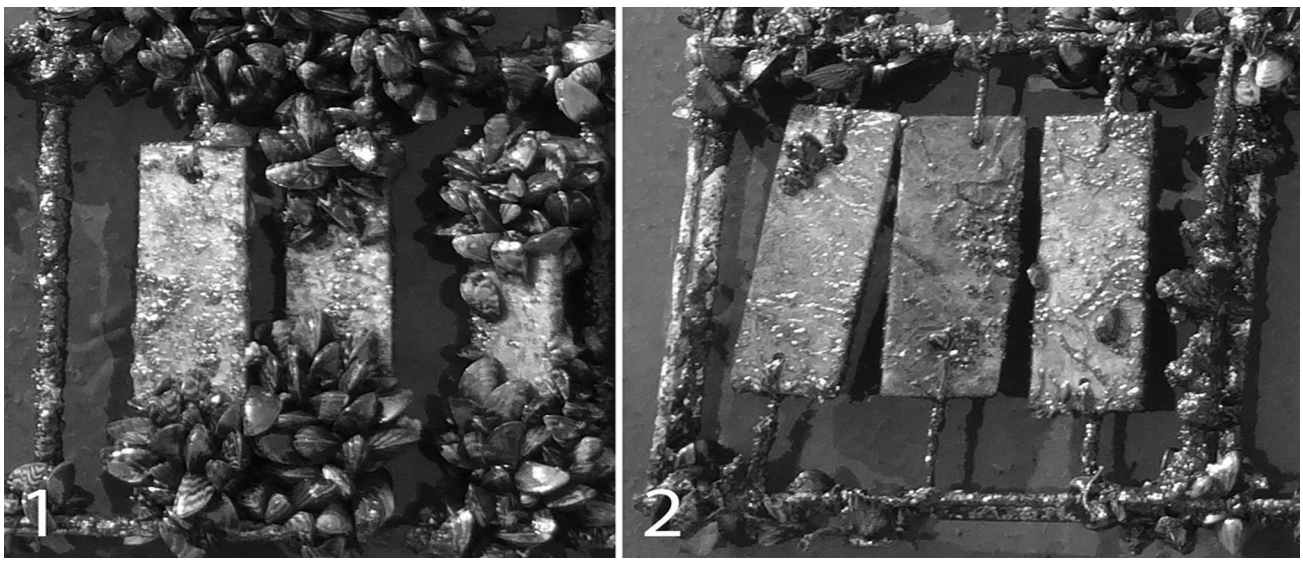

Fig. 12: Painted steel bars after 143-day exposure in the Dnipro River: 1—PP-115 (control coating), 2—PP-115/PyrC$_{12}$-DBS (16%)

DBS (16%) coatings. After 143-day exposure of experimental substrates in freshwater of the Dnipro River, the surface of PP-115/PyrC$_{12}$-DBS (16%) coatings showed almost a 13-fold reduction of total biomass formed by Dreissenidae mussels, compared with control substrates. For lower biocide content (8%), no difference in antifouling activity of modified and control coatings was detected. Overall, the obtained data indicate that the fabrication of contact-active protective coatings based on water-insoluble polymer matrix and water-insoluble biocide can be considered a promising approach to control biofouling in freshwater. However, relatively high biocide content is required to impart efficient antifouling activity to the coating.

Author contributions SR and OM were involved in conceptualization; J-FB and OP were involved in methodology and data curation; OM, J-FB, OD, OT, AH, AMD, and IM were involved in investigation; YL was involved in formal analysis; and SR and J-FB were involved in writing–original draft preparation.

Funding No funds, grants, or other support was received.

Data availability The authors declare that the data supporting the findings of this study are available within the paper. Should any raw data files be needed in another format they are available from the corresponding author upon reasonable request. Source data are provided with this paper.

Conflict of interest The authors declare that they have no conflict of interest. The authors have no competing interests to declare that are relevant to the content of this article.

References

1. Liu, D, Shu, H, Zhou, J, Bai, X, Cao, P, ''Research Progress on New Environmentally Friendly Antifouling Coatings in Marine Settings: A Review.'' *Biomimetics*, **8** (2) 200 (2023)
2. Del Grosso, CA, McCarthy, TW, Clark, CL, Cloud, JL, Wilker, JJ, ''Managing Redox Chemistry to Deter Marine Biological Adhesion.'' *Chem. Mater.*, **28** 6791–6796 (2016)
3. Faria, SI, Teixeira-Santos, R, Gomes, LC, Silva, ER, Morais, J, Vasconcelos, V, Mergulhão, FJM, ''Experimental Assessment of the Performance of Two Marine Coatings to Curb Biofilm Formation of Microfoulers.'' *Coatings*, **10** 893 (2020)
4. Tu, C, Chen, T, Zhou, Q, Liu, Y, Wei, J, Waniek, JJ, Luo, Y, ''Biofilm Formation and Its Influences on the Properties of Microplastics as Affected by Exposure Time and Depth in the Seawater.'' *Sci. Total Environ.*, **734** 139237 (2020)
5. Gormley, K, McLellan, F, McCabe, C, Hinon, C, Ferris, J, Kline, DI, Scott, BE, ''Automated Image Analysis of Offshore Infrastructure Marine Biofouling.'' *J. Mar. Sci. Eng.*, **6** 2 (2018)
6. Rao, TS, ''Biofouling in Industrial Water Systems.'' In: Amjad, Z, Demadis, KD (eds.) *Minerals Scales and Deposits*, pp. 123–140. Elsevier, New Jersey (2015)
7. Mathew, NT, Kronholm, J, Bertilsson, K, Despeisse, M, Johansson, B, ''Environmental and Economic Impacts of Biofouling on Marine and Coastal Heat Exchangers.'' In: Kishita, Y, Matsumoto, M, Inoue, M, Fukushige, S (eds.) *EcoDesign and Sustainability II. Sustainable Production, Life Cycle Engineering and Management*. Springer, Singapore (2021)
8. Liu, S, Kee, Y-H, Shang, B, Papanikolaou, A, ''Assessment of the Economic, Environmental and Safety Impact of Biofouling on a Ship's Hull and Propeller.'' *Ocean Eng.*, **285** 115481 (2023)
9. Lindholdt, A, Dam-Johansen, K, Olsen, SM, Yebra, DM, Kiil, S, ''Effects of Biofouling Development on Drag Forces of Hull Coatings for Ocean-Going Ships: A Review.'' *J. Coat. Technol. Res.*, **12** (3) 415–444 (2015)
10. Dong, M, Liu, L, Wang, D, Li, M, Yang, J, Chen, J, ''Synthesis and Properties of Self-Polishing Antifouling Coatings Based on BIT-Acrylate Resins.'' *Coatings*, **12** 891 (2022)
11. Olsen, SM, Yebra, DM, ''On the Use of the Term 'Self-Polishing' for Antifouling Paints.'' *Prog. Org. Coat.*, **76** 1699–1700 (2013)
12. Ytreberg, E, Lagerström, M, Nöu, S, Wiklund, A-K, ''Environmental Risk Assessment of Using Antifouling Paints on Pleasure Crafts in European Union Waters.'' *J. Environ. Manage.*, **281** 111846 (2021)
13. Lagerström, M, Ytreberg, E, Wiklund, A-K, ''Antifouling Paints Leach Copper in Excess–Study of Metal Release Rates and Efficacy Along a Salinity Gradient.'' *Water Res.*, **186** 116383 (2020)
14. Cima, F, Varello, R, ''Potential Disruptive Effects of Copper-Based Antifouling Paints on the Biodiversity of Coastal Macrofouling Communities.'' *Environ. Sci. Pollut. Res.*, **30** 8633–8646 (2023)
15. Miller, RJ, Adeleye, AS, Page, HM, Kui, L, Lenihan, HS, Keller, AA, ''Nano and Traditional Copper and Zinc Antifouling Coatings: Metal Release and Impact on Marine Sessile Invertebrate Communities.'' *J. Nanopart. Res.*, **22** 129 (2020)
16. Lagerström, M, Ferreira, J, Ytreberg, E, Eriksson-Wiklund, A-K, ''Flawed Risk Assessment of Antifouling Paints Leads to Exceedance of Guideline Values in Baltic Sea Marinas.'' *Environ. Sci. Pollut. Res.*, **27** 27674–27687 (2020)
17. Guardiola, FA, Cuesta, A, Meseguer, J, Esteban, MA, ''Risks of Using Antifouling Biocides in Aquaculture.'' *Int. J. Mol. Sci.*, **13** 1541–1560 (2012)
18. Onduka, T, Ojima, D, Ito, M, Ito, K, Mochida, K, Fujii, K, ''Toxicity of the Antifouling Biocide Sea-Nine 211 to Marine Algae, Crustacea, and a Polychaete.'' *Fish Sci.*, **79** 999–1006 (2013)
19. Silva, ER, Tulcidas, AV, Ferreira, O, Bayón, R, Igartua, A, Mendoza, G, Mergulhão, FJM, Faria, SI, Gomes, LC, Carvalho, S, Bordado, JCM, ''Assessment of the Environmental Compatibility and Antifouling Performance of an Innovative Biocidal and Foul-release Multifunctional Marine Coating.'' *Environ. Res.*, **198** 111219 (2021)
20. Machate, O, Dellen, J, Schulze, T, Wentzky, VC, Krauss, M, Brack, W, ''Evidence for Antifouling Biocides as One of the Limiting Factors for the Recovery of Macrophyte Communities in Lakes of Schleswig-Holstein.'' *Environ. Sci. Eur.*, **33** 57 (2021)
21. Lewis, K, Klibanov, AM, ''Surpassing Nature: Rational Design of Sterile-Surface Materials.'' *Trends Biotechnol.*, **23** (7) 343–348 (2005)
22. Cuervo-Rodríguez, R, López-Fabal, F, Gómez-Garcés, JL, Muñoz-Bonilla, A, Fernández-García, M, ''Contact Active Antimicrobial Coatings Prepared by Polymer Blending.'' *Macromol. Biosci.*, **17** 1700258 (2017)
23. Izmaylov, B, Di Gioia, D, Markova, G, Aloisio, I, Colonna, M, Vasnev, V, ''Imidazolium Salts Grafted on Cotton Fibers for Long-Term Antimicrobial Activity.'' *React. Funct. Polym.*, **87** 22–28 (2015)
24. Poverenov, E, Klein, M, ''Formation of Contact Active Antimicrobial Surfaces by Covalent Grafting of Quaternary Ammonium Compounds.'' *Colloids Surf. B: Biointerfaces*, **169** 195–205 (2018)
25. Reddy, GKK, Nancharaiah, YV, ''Alkylimidazolium Ionic Liquids for Biofilm Control: Experimental Studies on Controlling Multispecies Biofilms in Natural Waters.'' *J. Mol. Liq.*, **336** 116859 (2021)
26. Cornellas, A, Perez, L, Comelles, F, Ribosa, I, Manresa, A, ''Self-Aggregation and Antimicrobial Activity of Imida-

zolium and Pyridinium Based Ionic Liquids in Water Solutions.'' *J. Colloid Interface Sci.*, **355** 164–171 (2011)
27. Vereshchagin, AN, Frolov, NA, Egorova, KS, Seitkalieva, MM, Ananikov, VP, ''Quaternary Ammonium Compounds (QACs) and Ionic Liquids (ILs) as Biocides: From Simple Antiseptics to Tunable Antimicrobials.'' *Int. J. Mol. Sci.*, **22** 6793 (2021)
28. Bergamo, VZ, Donato, RK, Dalla Lana, DF, Donato, KJZ, Ortega, GG, Schrekker, HS, Fuentefria, AM, ''Imidazolium Salts as Antifungal Agents: Strong Antibiofilm Activity Against Multidrug-Resistant *Candida tropicalis* Isolates.'' *Lett. Appl. Microbiol.*, **60** 66–67 (2014)
29. Reddy, GKK, Nancharaiah, YV, Venugopalan, VP, ''Long Alkyl-Chain Imidazolium Ionic Liquids: Antibiofilm Activity Against Phototrophic Biofilms.'' *Colloids Surf. B. Biointerfaces.*, **155** 487–496 (2017)
30. Semenyuta, I, Trush, M, Kovalishyn, V, Rogalsky, S, Hodyna, D, Karpov, P, Xia, Z, Tetko, I, Metelytsia, L, ''Structure-Activity Relationship Modeling and Experimental Validation of the Imidazolium and Pyridinium Based Ionic Liquids as Potential Antibacterials of MDR *Acinetobacter baumannii* and *Staphylococcus aureus.*'' *Int. J. Mol. Sci.*, **22** 563 (2021)
31. Gilbert, P, Moore, LE, ''Cationic Antiseptics: Diversity of Action Under a Common Epithet.'' *J. Appl. Microbiol.*, **99** 703–715 (2005)
32. Tischer, M, Pradel, G, Ohlsen, K, Holzgrabe, U, ''Quaternary Ammonium Salts and Their Antimicrobial Potential: Targets or Nonspecific Interactions?'' *Chem. Med. Chem.*, **7** 22–31 (2012)
33. Reddy, GKK, Rajitha, K, Nancharaiah, YV, ''Antibiofouling Potential of 1-Alkyl-3-Methylimidazolium Ionic Liquids: Studies Against Biofouling Barnacle Larvae.'' *J. Mol. Liq.*, **302** 112497 (2020)
34. Piazza, V, Dragić, I, Cepčić, K, Faimali, M, Garaventa, F, Turk, T, Berne, S, ''Antifouling Activity of Synthetic Alkylpyridinium Polymers Using the Barnacle Model.'' *Mar. Drugs*, **12** 1959–1976 (2014)
35. Siedenbiedel, F, Tiller, JC, ''Antimicrobial Polymers in Solution and on Surfaces: Overview and Functional Principles.'' *Polymers*, **4** 46–71 (2012)
36. Walczak, M, Richert, A, Burkowska-But, A, ''The Effect of Polyhexamethylene Guanidine Hydrochloride (PHMG) Derivatives Introduced into Polylactide (PLA) on the Activity of Bacterial Enzymes.'' *J. Ind. Microbiol. Biotechnol.*, **41** 1719–1724 (2014)
37. Rogalsky, S, Bardeau, J-F, Wu, H, Lyoshina, L, Bulko, O, Tarasyuk, O, Makhno, S, Cherniavska, T, Kyselov, Y, Koo, JH, ''Structural, Thermal and Antibacterial Properties of Polyamide 11/Polymeric Biocide Polyhexamethylene Guanidine Dodecylbenzenesulfonate Composites.'' *J. Mater. Sci.*, **51** 7716–7730 (2016)
38. Ghamrawi, S, Bouchara, J-P, Tarasyuk, O, Rogalsky, S, Lyoshina, L, Bulko, O, Bardeau, J-F, ''Promising Silicones Modified with Cationic Biocides for the Development of Antimicrobial Medical Devices.'' *Mater. Sci. Eng. C*, **75** 969–979 (2017)
39. Swiontek Brzezinska, M, Walczak, M, Jankiewizs, U, Pejchalová, M, ''Antimicrobial Activity of Polyhexamethylene Guanidine Derivatives Introduced into Polycaprolactone.'' *J. Polym. Environ.*, **26** (2) 589–595 (2018)
40. Moshynets, O, Bardeau, J-F, Tarasyuk, O, Makhno, S, Cherniavska, T, Dzhuzha, O, Potters, G, Rogalsky, S, ''Antibiofilm Activity of Polyamide 11 Modified with Thermally Stable Polymeric Biocide Polyhexamethylene Guanidine 2-Naphtalenesulfonate.'' *Int. J. Mol. Sci.*, **20** (2) 348 (2019)
41. Nigmatullin, R, Gao, F, Konovalova, V, ''Permanent, Non-Leaching Antimicrobial Polyamide Nanocomposites Based on Organoclays Modified with a Cationic Polymer.'' *Macromol. Mater. Eng.*, **294** 795–805 (2009)
42. Inásio, ÂS, Domingues, NS, Nunes, A, Martins, PT, Moreno, MJ, Estronca, LM, Fernandes, R, Moreno, AJM, Borrego, MJ, Gomes, JP, Vaz, WLC, Vieira, OV, ''Quaternary Ammonium Surfactant Structure Determines Selective Toxicity Towards Bacteria: Mechanism of Action and Clinical Implications in Antibacterial Prophylaxis.'' *J. Antimicrob. Chemother.*, **71** 641–654 (2016)
43. Trush, M, Metelytsia, L, Semenyuta, I, Kalashnikova, L, Papeykin, O, Venger, I, Tarasyuk, O, Bodachivska, L, Blagodatnyi, V, Rogalsky, S, ''Reduced Ecotoxicity and Improved Biodegradability of Cationic Biocides Based on Ester-Functionalized Pyridinium Ionic Liquids.'' *Environ. Sci. Poll. Res.*, **26** (5) 4878–4889 (2019)
44. Cao, Y, Cen, Y, Sun, X, Mu, T, ''Quantification of Ionic Liquids Concentration in Water and Qualification of Conjugated and Inductive Effects of Ionic Liquids by UV Spectroscopy.'' *Clean Soil Air Water*, **42** 1162–1169 (2014)
45. Volynets, GP, Barthels, F, Hammerschmidt, SJ, Moshynets, OV, Lukashov, SS, Starosyla, SA, Vyshniakova, HV, Iungin, OS, Bdzhola, VG, Prykhodko, AO, Syniugin, AR, Sapelkin, VM, Yarmoluk, SM, Schirmeister, T, ''Identification of Novel Small-Molecular Inhibitors of *Staphylococcus aureus* Sortase A Using Hybrid Virtual Screening.'' *J. Antibiot.*, **75** 321–332 (2022)
46. Protasov, A, Bardeau, J-F, Morozovskaya, I, Boretska, M, Cherniavska, T, Petrus, L, Tarasyuk, O, Metelytsia, L, Kopernik, I, Kalashnikova, L, Dzhuzha, O, Rogalsky, S, ''New Promising Antifouling Agent Based on Polymeric Biocide Polyhexamethylene Guanidine Molybdate.'' *Environ. Toxicol. Chem.*, **36** (9) 2543–2551 (2017)
47. Potangale, M, Das, A, Kapoor, S, Tiwari, S, ''Effect of Anion and Alkyl Chain Length on the Structure and Interactions of N-Alkyl Pyridinium Ionic Liquids.'' *J. Mol. Liq.*, **240** 694–707 (2017)
48. Mokti, N, Borhan, A, Nur, S, Zaine, A, Fatimah, H, Zaid, M, ''Synthesis and Characterisation of Pyridinium-Based Ionic Liquid as Activating Agent in Rubber Seed Shell Activated Carbon Production for CO_2 Capture.'' *J. Adv. Res. Fluid Mech. Therm. Sci.*, **82** 85–95 (2021)
49. Bardeau, J-F, Parikh, AN, Beers, JD, Swanson, BI, ''Phase Behavior of a Structurally Constrained Organic-Inorganic Crystal: Temperature-Dependent Infrared Spectroscopy of Silver n-Dodecanethiolate.'' *J. Phys. Chem. B*, **104** 627–635 (2000)
50. Xu, ZP, Braterman, PS, ''High Affinity of Dodecylbenzene Sulfonate for Layered Double Hydroxide and Resulting Morphological Changes.'' *J. Mater. Chem.*, **13** 268–273 (2003)
51. Sperline, RP, Yuan Song, Y, Freiser, H, ''Fourier Transform Infrared Attenuated Total Reflection Linear Dichroism Study of Sodium Dodecylbenzenesulfonate Adsorption at the Al_2O_3/Water Interface Using Al_2O_3-Coated Optics.'' *Langmuir*, **10** 31–44 (1994)
52. Shishlov, NM, Khursan, SL, ''Effect of Ion Interactions on the IR Spectrum of Benzenesulfonate Ion. Restoration of Sulfonate Ion Symmetry in Sodium Benzenesulfonate Dimer.'' *J. Mol. Struct.*, **1123** 360–366 (2016)
53. Bumbac, M, Zaharescu, T, Nicolescu, CM, ''Thermal and Radiation Stability of Alkyd Based Coatings Used as Insulators in the Electrical Rotating Machines.'' *J. Sci. Arts*, **1** (38) 119–130 (2017)

54. Jones, GC, Jackson, B, *Infrared Transmission Spectra of Carbonate Minerals*. Springer, Dordrecht, Netherlands (1993)
55. White, WB, ''The Carbonate Minerals.'' In: Farmer, VC (ed.) *The Infrared Spectra of Minerals*, pp. 227–284. Mineralogical Society of London (1974)
56. Badou, A, Pont, S, Auzoux-Bordenave, S, Lebreton, M, Bardeau, J-F, ''New Insight on Spatial Localization and Microstructures of Calcite-Aragonite Interfaces in Adult Shell of *Haliotis tuberculata*: Investigations of Wild and Farmed Abalones by FTIR and Raman Mapping.'' *J. Struct. Biol.*, **214** 107854 (2022)
57. Zhang, Y, He, H, Zhang, S, Fan, M, ''Hydrogen-Bonding Interactions in Pyridinium-Based Ionic Liquids and Dimethyl Sulfoxide Binary Systems: A Combined Experimental and Computational Study.'' *ACS Omega*, **3** (2) 1823–1833 (2018)
58. Law, K-Y, ''Definitions for Hydrophilicity, Hydrophobicity, and Superhydrophobicity: Getting the Basics Right.'' *J. Phys. Chem. Lett.*, **5** 686–688 (2014)
59. Pardo, IJ, van der Ven, LGJ, van Benthem, RATM, de With, G, Esteves, ACC, ''Hydrophilic Self-replenishing Coatings with Long-term Water Stability for Anti-Fouling Applications.'' *Coatings*, **8** 184 (2018)
60. Pistone, A, Scolaro, C, Visco, A, ''Mechanical Properties of Protective Coatings Against Marine Fouling: A Review.'' *Polymers*, **13** 173 (2021)
61. Qiu, H, Feng, K, Gapeeva, A, Meurisch, K, Kaps, S, Li, X, Yu, L, Mishra, YK, Adelung, R, Baum, M, ''Functional Polymer Materials for Modern Marine Biofouling Control.'' *Prog. Polym. Sci.*, **127** 101516 (2022)
62. Moshynets, OV, Spiers, AJ, ''Viewing Biofilms Within the Larger Context of Bacterial Aggregations.'' In: Dhanasekaran, D, Thajuddin, N (eds.). *Microbial Biofilms–Importance and Applications*, pp 3-22. InTech Press (2016). https://doi.org/10.5772/61499
63. Ong, KS, Mawang, CI, Daniel-Jambun, D, Lim, YY, Lee, SM, ''Current Anti-Biofilm Strategies and Potential of Antioxidants in Biofilm Control.'' *Expert Rev. Anti-Infect. Ther.*, **16** 855–864 (2018)
64. Liu, X, Tong, W, Wu, Z, Jiang, W, ''Poly(N-vinylpyrrolidone)-Grafted Poly(dimethylsiloxane) Surfaces with Tunable Microtopography and Anti-Biofouling Properties.'' *RSC Adv.*, **3** 4716–4722 (2013)
65. Kalia, VC, ''Quorum Sensing Inhibitors: An Overview.'' *Biotechnol. Adv.*, **31** 224–245 (2013)
66. Bhattarai, HD, Ganti, VS, Paudel, B, Lee, YK, Hong, Y-K, Shin, HW, ''Isolation of Antifouling Compounds from the Marine Bacterium, *Shewanella Oneidensis* SCH0402.'' *World J. Microbiol. Biotechnol.*, **23** 243–249 (2007)
67. Bazes, A, Silkina, A, Douzenel, P, Faÿ, F, Kervarec, N, Morin, D, Berge, J-P, Bourgougnon, N, ''Investigation of the Antifouling Constituents from the Brown Alga *Sargassum Muticum* (Yendo) Fensholt.'' *J. Appl. Phycol.*, **21** 395–403 (2009)